Dark Matter Candidates

Rose Grey, Gabriël Koole, Davey Oogjes and Samuel van Beek

June 21, 2018

Abstract

Our beautiful abstract will come here.

Contents

1 Introduction (Gabriël)

One of the most important problems in particle physics and cosmology is the nature of dark matter (DM) in the Universe. Evidence for the existence of large amounts of DM in the Universe has been increasing steadily over last decades, yet its origin and nature remain unknown at this time. A popular view on dark matter is that is consists of weakly interacting massive particles (WIMPs). This is a popular DM candidate for a number of reasons. First of all, in many theoretically well-motivated extensions of the Standard Model (SM) WIMPs arise naturally. In addition, WIMPs are attractive experimentally because their detection rates are within reach of current or future detectors [1]. The third and perhaps most enticing feature of WIMPs as a DM can didate is that the production mechanism of the DM abundance today, the *thermal freeze out* mechanism, is simple and understood entirely [2]. The freeze out mechanism will be discussed in section 2.2. The beauty of this mechanism is emphasised by the so-called the *WIMP miracle*. To account for the amount of DM in the Universe today, the freeze out mechanism provides constraints on the mass and the cross section of the WIMP. Using the observed DM abundance today, a particle with a mass in the range of tens-hundreds GeV and a cross section which corresponds to weak interaction is predicted [3]. These properties coincide with the expected properties of the lightest stable particle (LSP) in many supersymmetric (SUSY) models. An LSP like the lightest neutralino $\tilde{X}_1^0$ is therefore an excellent WIMP candidate [4]. The seemingly magical correlation between the DM problem and SUSY models, which were initially proposed as a solution to the hierarchy problem in the SM, is therefore named the WIMP miracle. The properties of the lightest neutralino as a DM candidate will be discussed in section 2.3.

Besides the neutralino in SUSY models, other beyond the Standard Model (BSM) theories provide other WIMP candidates. One of these theories suggests the existence of an extra spatial dimension. This extra dimension takes several forms, but this review focuses on the DM candidate coming from a universal extra dimension (UED). In UED the 5-dimensional spacetime is reduced to the 4-dimensional spacetime using the Kaluza-Klein (KK) method. It was initially motivated to unify electromagnetism with gravity, although it has had influence in many other fields of physics. The DM candidate that arises in these models is known as the lightest Kaluza-Klein particle (LKP). See section 2.4 for a more detailed discussed of UED.

Although WIMPs are a very popular DM candidate, conclusive evidence has not been discovered yet. Therefore alternative theories on DM remain relevant. A widely discussed non-WIMP which could explain the nature of DM is the Axion [5]. Also, models of Primordrial Black Holes (PBHs) as a DM candidate have received attention, for an excellent discussion of PBHs see [6].

This review is organized as follows. In section 2 WIMPs are discussed starting with the general properties (2.1), followed by the freeze out mechanism (2.2), WIMPs in supersymmetric (SUSY) models (2.3), the LKP in universal extra dimension models (2.4) and constraints on WIMIPs from collider searches (2.5). Section 3 gives on overview of non-WIMPs such as sterile neutrinos (3.1), axions (3.2) and fuzzy dark matter (3.3).

2 WIMPs

2.1 Properties of WIMPs (Rose)

As DM constitutes $\sim$85% of the matter in our universe, a pressing question to ask ourselves: what is DM actually made of? Through observations, various properties of these particles have been deduced, which leads us to rule out a family of candidates. However, there is still a large number of possible candidates, with masses ranging from 10^{-5} eV to 10^4 $M_\odot$ [7]. One particular model is known as WIMPs. This has properties as follows:

- *Massive.*

  Their effects were historically noticed when the calculation of the angular momentum of the galaxy was smaller than the observed result. This is because the calculations used a mass approximation from all observable stars, with an average estimation for the bodies orbiting them. It was concluded that there must be matter we cannot see, hence the terminology Dark Matter. It is considered to reside in a halo around the galaxy. Generally, they are said to have masses in the range of 10 GeV $\sim$ 1 TeV [7].

- *Cold.*

  Here the term cold means non-relativistic. DM has also been attributing some contribution towards structure formation, where massive non-relativistic particles will allow structure to form hierarchically [8]. DM will cause small particles to gravitationally collapse, which in turn will pull more and more objects until large-scale structures are formed. The theory for cold DM has been solidified due to advancements with the Lamba-CDM model [9].

- *Non-baryonic.*

  The root cause for the non-baryonic property is still an ongoing investigation in DM physics. Measurements for the current energy density of baryonic matter has almost all of the baryonic matter accounted for in luminous objects. There is a large deficit for an explanation for non-baryonic objects in luminous matter [10]. This also leads us to believe that our non-luminous matter is non-baryonic.

- *Weakly Interacting.*

  Constraints have been put on the WIMP cross-section, roughly in the range of $10^{-28} - 10^{-23}$ [11]. Combining this with the mass constraint, this is the behaviour we would expect from a weakly interacting particle.

- *Electrically Neutral.*

  This is synonymous with being dark. If they are not electrically neutral, they would interact with photons and emit light that we would be able to detect.

- *Stable.*

  It should go without saying any DM particle must be stable. We assume that DM has been around since the beginning of time, having a similar abundance as that of the abundance at the time of its freeze-out. If these particles could

decay, they would have all decayed after ∼14 billion years, and their effects would not be visible today.

The above properties describe a family of candidates known as WIMPs. Although the finer details of these particles will be different from model to model, these basic properties have been well implemented. They are a new fundamental particle and are an addition to the SM. Some basic models are particles arising from supersymmetry and a universal extra dimension, as well as a particle known as the Little Higgs [12].

2.2 The freeze out mechanism (Gabriël)

As briefly mentioned in the introduction the freeze out mechanism is the production mechanism of the WIMP DM abundance today. In the early Universe the WIMP, denoted as X, and the SM particles were in close contact at high temperatures $(T \gg m_X)$. The cosmological plasma (containing the SM particles) and the DM were in thermal equilibrium due to DM particle production from annihilations [1]. The annihilation rate is given by $\Gamma_{\mathrm{ann}} = n_X \langle \sigma_{\mathrm{ann}} v \rangle$ where n_X is the number density of DM particles, and $\langle \sigma_{\mathrm{ann}} v \rangle$ thermally averaged product of the annihilation cross section and the velocity [13]. A freeze out is defined as the inability of annihilations to keep the particle in thermal equilibrium [14]. The freeze out, or thermal decoupling, of DM occurred when the annihilation rate became smaller than the expansion rate of the Universe $\Gamma_{\mathrm{ann}} \lesssim H$. In other words, the DM particles were being separated by the expansion of the Universe faster than they could annihilate to maintain equilibirium, resulting in a freeze out and a relic density of DM WIMPs. Using this mechanism we can calculate this relic density of DM.

We start with the the Boltzmann equation for the DM number density n_X and the law of entropy conservation:

$$\frac{dn_X}{dt} = -3Hn_X - \langle \sigma_{\mathrm{ann}} v \rangle \{ n_X - n_X^{(0)} \}, \tag{1}$$

$$\frac{ds}{dt} = -3Hs, \tag{2}$$

where t is time, s is the entropy density, H is the Hubble constant, and $n_X^{(0)}$ is the equilibrium density [15]. Equation 1 and 2 can be combined into a single equation. Defining $Y \equiv n_X/s = n_X/T^3$, the WIMP yield, the Boltzmann equation for a DM particle becomes:

$$\frac{dY}{dt} = T^3 \langle \sigma_{\mathrm{ann}} v \rangle \{ Y_{\mathrm{EQ}}^2 - Y^2 \}, \tag{3}$$

where $Y_{\mathrm{EQ}} = n_X^{(0)}/T^3$ [14]. In the literature this equation is often rewritten in terms of a new variable $x \equiv m_X/T$ for convenience. Equation 3 then becomes:

$$\begin{aligned}
\frac{dY}{dx} &= \frac{1}{3H} \frac{ds}{dx} \{ Y^2 - Y_{\mathrm{EQ}}^2 \} \\
&= -\frac{\lambda}{x^2} \{ Y^2 - Y_{\mathrm{EQ}}^2 \}.
\end{aligned} \tag{4}$$

Here, λ is the ratio of the annihilation rate to the expansion rate:

$$\lambda \equiv \frac{m_X^3 \langle \sigma_{\text{ann}} v \rangle}{H(m_X)}, \tag{5}$$

where $H(m_X) = Hx^2$ in the radiation era where dark matter production typically occurs [14]. Since the DM particles are relativistic in this era, $x \gg 1$, the equilibrium abundance Y_{EQ} will exponentially suppressed. Therefore equation 4 simplifies to:

$$\frac{dY}{dx} \simeq -\frac{\lambda Y^2}{x^2}. \tag{6}$$

Integrating this from the freeze out (Y_{fo}) to late times (Y_∞) and using the fact that typically $Y_{\text{fo}} \gg Y_\infty$), the DM abundance today becomes $Y_\infty \simeq x_{\text{fo}}/\lambda$. The number density at late times is $Y_\infty T^3$, so the energy density of DM today can be expressed as:

$$\rho_X = m_X Y_\infty T^3 \simeq \frac{m_X Y_\infty T_0^3}{30}, \tag{7}$$

where T_0 is the temperature today [14]. Using the expression for Y_∞, the DM abundance $\Omega_X h^2$ can be derived:

$$\begin{aligned}
\Omega_X h^2 \equiv \frac{\rho_X h^2}{\rho_c} &= \frac{m_X Y_\infty T_0^3 h^2}{30 \rho_c} \\
&= \frac{x_{\text{fo}}}{\lambda} \frac{m_X T_0^3 h^2}{30 \rho_c} \\
&= \frac{x_{\text{fo}}}{m_X^2 \langle \sigma_{\text{ann}} v \rangle} \frac{T_0^3 h^2 H(m_X)}{30 \rho_c}.
\end{aligned} \tag{8}$$

where ρ_c is the critical density. Finally the Hubble rate at freeze out $H(m_X)$ can be calculated (see [14]) and the quantities $T_0 \simeq 2.35 \times 10^{-13}$ GeV and $\rho_c \simeq 8 \times 10^{-47} h^2$ GeV^4 are known [1]. It is now possible to find the value of $\langle \sigma_{\text{ann}} v \rangle$ for a given WIMP mass for which $\Omega_X h^2$ is in agreement with the mearued value $\Omega_{\text{CDM}} h^2 = 0.1120 \pm 0.0056$ [16]. Figure 1 shows the abundance of the WIMP versus x. Many experiments aim to put constraints on the values of the WIMP mass and annihilation cross section using the freeze out mechanism. Some of these experimental constraints will be discussed in section 2.5.

2.3 SUSY (Samuel)

In many theories for physics beyond the Standard Model, supersymmetry is an important feature. One of the motivations that supersymmetry could provide answers on the nature of dark matter is that a combination of supersymmetric transformations leads to a spacetime transformation. Subsequently, theories of local supersymmetry necessarily contain local spacetime transformations and thus contain gravity [7]. Dark matter is subject to gravitational forces and therefore supersymmetry is an interesting study area to investigate dark matter.

One important ingredient in supersymmetric dark matter is R-parity. This discrete symmetry can be written as $R = (-1)^{3(B-L)+2S}$. Here, B is the baryon number,
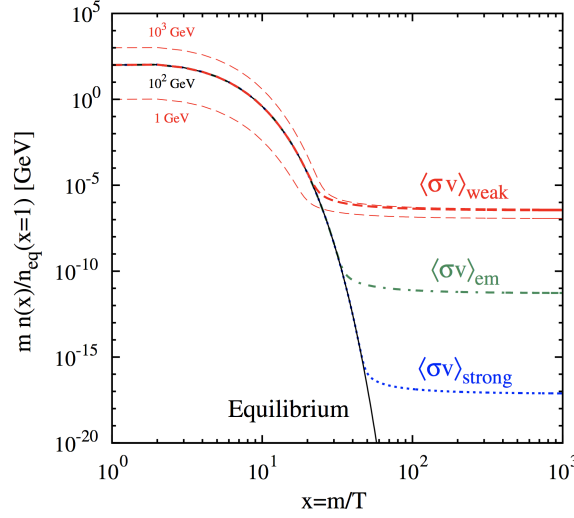
Figure 1: Evolution of the cosmological WIMP abundance as a function of $x = m/T$. Note that the y axis spans 25 orders of magnitude. The thick curves show the WIMP mass density, normalised to the initial equilibrium number density, for different choices of annihilation cross section $\langle \sigma_{\text{ann}} v \rangle$ and mass m. Results for m $m = 100$ GeV are shown for weak interactions, $\langle \sigma_{\text{ann}} v \rangle = 2 \times 10^{-26} \text{cm}^3 \text{s}^{-1}$, (dashed red), electromagnetic interactions, $\langle \sigma_{\text{ann}} v \rangle = 2 \times 10^{-21} \text{cm}^3 \text{s}^{-1}$ (dot-dashed green), and strong interactions, $\langle \sigma_{\text{ann}} v \rangle = 2 \times 10^{-15} \text{cm}^3 \text{s}^{-1}$ (dotted blue). For the weak cross section the thin dashed curves show the WIMP mass dependence for $m = 10^3$ GeV (upper dashed curve) and $m = 1$ GeV (lower dashed curve). The solid black curve shows the evolution of the equilibrium abundance for $m = 100$ GeV. Figure taken from [16].

L the lepton number and S the spin. Regarding SM particles, $R = 1$ and for supersymmetric partner particles $R = $-1. In case of R-parity violation, no selection rules exist that would prevent the decay of the supersymmetric particles to particles of the order of a few GeV. However, no stable supersymmetric particles could exist if all these particles decay. Therefore, only supersymmetry with invariant R-parity is considered. This provides a lightest R-odd particle that is stable and does not decay to other SM or SUSY particles. This particular particle is called the lightest supersymmetric particle (LSP).

In the minimal supersymmetric extension of the Standard Model, there is a successful gauge coupling unification. The term *minimal* refers to the limit on the superpartner masses of a few TeV [17], which is already quite heavy compared to Standard Model particles. The extension consists of adding supersymmetric partners that corresponds to the fields of the Higgs doublet extension in the Standard Model [18]. A Standard Model particle together with it's corresponding superpartner together form a supermultiplet. In Table 1 the MSSM particles are listed together with their quantum numbers.

The superpartners of the W-boson and the charged Higgs bosons are the charged higgsino and gaugino. The same SU(3) x U(1) quantum numbers are associated with the supersymmetric particles. Hence, mixing will occur after electroweak-symmetry breaking. Linear combinations provide mass eigenstates that are known as *charginos*

Table 1: Overview of the fields in the MSSM together with the associated SU(3) $\otimes$ SU(2) $\otimes$ U(1) quantum numbers. Only the first generation of particles is considered regarding quarks and leptons [18]

Field Content of the MSSM						
Super-multiplets	Super-field	Bosonic fields	Fermionic partners	SU(3)	SU(2)	U(1)
gluon/gluino	$\widehat{V}_8$	g	$\widetilde{g}$	8	1	0
gauge/	$\widehat{V}$	$W^{\pm}, W^0$	$\widetilde{W}^{\pm}, \widetilde{W}^0$	1	3	0
gaugino	$\widehat{V}'$	B	$\widetilde{B}$	1	1	0
slepton/	$\widehat{L}$	$(\widetilde{\nu}_L, \widetilde{e}_L^-)$	$(\nu, e^-)_L$	1	2	-1
lepton	$\widehat{E}^c$	$\widetilde{e}_R^-$	e_R^-	1	1	-2
squark/	$\widehat{Q}$	$(\widetilde{u}_L, \widetilde{d}_L)$	$(u, d)_L$	3	2	$1/3$
quark	$\widehat{U}^c$	$\widetilde{u}_R$	u_R	3	1	$4/3$
	$\widehat{D}^c$	$\widetilde{d}_R$	d_R	3	1	$-2/3$
Higgs/	$\widehat{H}_d$	(H_d^0, H_d^-)	$(\widetilde{H}_d^0, \widetilde{H}_d^-)$	1	2	-1
higgsino	$\widehat{H}_u$	(H_u^+, H_u^0)	$(\widetilde{H}_u^+, \widetilde{H}_u^0)$	1	2	1

($\chi_1^{\pm}$). Furthermore, the superpartners of the photon, the Z-boson and the neutral Higgs boson (the photino, zino and neutral higgsino respectively) generally mix into four mass eigenstates called *neutralinos* ($\chi_1^0, \chi_2^0, \chi_3^0, \chi_4^0$). The lightest of these four supersymmetric particles, χ_1^0, would be the LSP in the MSSM and weakly interacting. Therefore the neutralino is a considerable dark matter-candidate. The other neutralinos and the charginos may decay into the lightest neutralino.

2.3.1 The neutralino

The mass eigenstate of the neutralino can be written as a linear combination of neutral higgsinos, the wino and the bino [7]. The bino is a U(1) superpartner of the corresponding to weak hypercharge. It is the lightest gaugino [19], a superpartner of a gauge field.

$$\tilde{\chi}^0 = N_{10}\tilde{B} + N_{20}\tilde{W}^3 + N_{30}\tilde{H}_1^0 + N_{40}\tilde{H}_2^0 \tag{9}$$

Here, N_{i0} are coefficients that are determined by diagonalization of the mass matrix of the neutralino. The subscript 0 denotes that the lightest of the four possible neutralinos is considered. $\tilde{B}, \tilde{W}^3, \tilde{H}_i^0$ are the superpartners mentioned above.

2.3.2 Neutralino production and annihilation

The simplest process for neutralino production is through electron-positron annihilation resulting in a neutralino pair via the Z^0 resonance. Neutralinos can annihilate into many final states. The most important states are the states that are present in lowest order perturbation theory. Possible states are fermion-antifermion pairs

and combinations of the W-bosons, Z-boson or Higgs bosons. To study the neutralinos, the annihilation cross-section in the non-relativistic case is needed. The cross-section σ_A can be written as

$$\sigma_A v = a + bv^2 + \mathcal{O}(v^4) \tag{10}$$

with a the s-wave contribution if velocity v is zero. Both contributions from s and p-waves are contained in b. For s-waves angular momentum $l = 0$, for p-waves $l = 1$. At low energies, the scattering amplitudes of particles are independent of the angle. Neutralinos in the galaxy move relatively slow $\sim 0.001c$ [7], meaning that only a is needed for calculations regarding relic neutralinos. During the freeze-out, however, the neutralinos moved with speeds around 0.5c. In short, if $a >> b$, then $\langle \sigma_A v \rangle = a$. If $a << b$, then $\langle \sigma_A v \rangle \approx 6b/x_f$, with $x_f = T_f/m_\chi$, which is the case at freezeout [7]. Therefore, both a and b are needed for calculations. For all possible decay product of the neutralino, the a and b contributions have been calculated [7].

As an example, the neutralino could annihilate to weak gauge bosons when the mass is high enough, i.e. $m_\chi > m_W$. It was found that annihilation to a W/Z-boson pair is not subject to s-wave suppressions mechanisms, making neutralinos important for these pair productions in case the neutralinos are heavy enough [20]. Multiple annihilation processes are possible regarding W/Z-bosons. In Figures 2 and 3 the Feynman diagrams for these processes are shown.
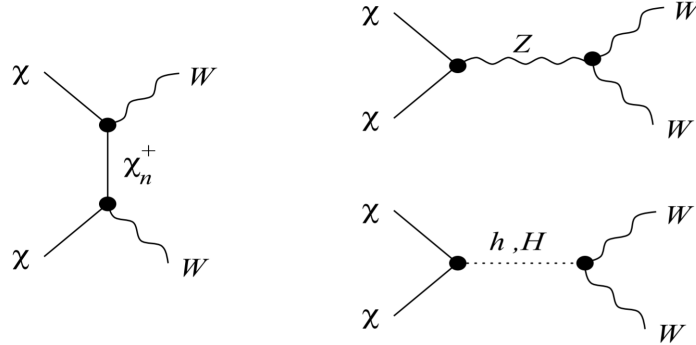

Figure 2: Feynman diagrams for neutralino annihilation and W-boson pair creation via chargino, Z-boson or Higgs boson [7]
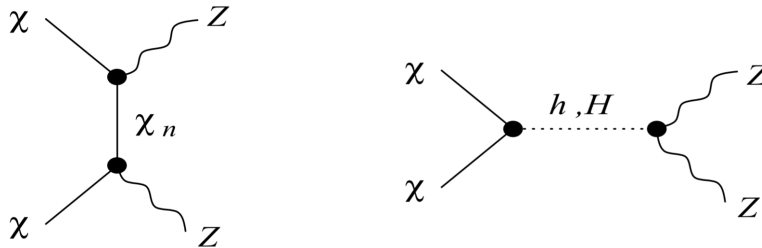
.

Figure 3: Feynman diagrams for neutralino annihilation and Z-boson pair creation, via neutralino or Higgs boson

Similar processes are found for the other final states. Many channels are closed

or suppressed due to too light neutralino masses. Therefore, fermionic final states are often the channels that are open.

2.3.3 Interactions involving neutralinos

Neutralinos do not have vector interactions with other particles, since neutralinos are Majorana fermions (neutralino is it's own anti-particle) [7]. Therefore, only spin-spin interactions and scalar interactions are considered. The total elastic-scattering cross-section is the sum of the two types of interaction of the neutralino.

The spin interaction of a neutralino with another particle's spin is an axial-vector interaction. The scalar interaction is between the mass of the neutralino and a nucleon's mass.

2.4 Universal Extra Dimension (Rose)

Although the neutralino is a strong candidate as a DM particle, while the identity of the DM particle remains unknown we will also probe alternative theories. One of these theories is the existence of an extra spatial dimension. This spatial dimension would arise at a high energy scale. The idea is motivated by string theory and M-Theory. Although these will not be discussed at length in this review; an excellent reference for this would be [21].

This has multiple benefits to the standard model, including anomaly cancellation, dynamical electroweak symmetry breaking, prevention of rapid proton decay and, for the importance of this review, a DM candidate [22]. This extra dimension takes several forms. Firstly there is a universal extra dimension (UED) [23], in which all particles in the Standard Model will propagate on. Alternatively, our observable (3+1) dimensional space is a brane existing in a higher $(3+\delta+1)$ bulk spacetime [24]. In the Arkani-Hamed, Dimopoulos and Dvali (ADD) model, all Standard Model particles will propagate on 3 spatial dimensions whereas the graviton will propagate in the bulk. There are also intermediate theories, where only certain families will propagate in the bulk, which gives rise to the anomaly cancellations [25]. We could also consider a warped extra dimension, a dimension with a non-factorisable, 'warped', geometry [26]. For the remainder of this review we shall be focusing on UED.

UED offers an additional feature not seen in the brane approach. There is remains translational symmetry, leading to a conservation of the momentum in all dimensions. In UED, the extra spatial dimension is flat space compactified onto S^1. The method used to reduce the 5-dimensional theory to the 4-dimensional one is known as Kaluza Klein (KK) reduction, which gives a number of interesting properites. We will give a brief, simplified description of this shortly. To account for chiral fermions, a Z_2 symmetry needs to be imposed, i.e. $x^4 \rightarrow -x^4$. Fields can be even or odd under this symmetry. The compactified space is therefore known as an S^1/Z_2 orbifold [27]. We will have orbifold fixed points at $x^4 = 0, \pi R$. These fixed points will break translational symmetry in the x^5 direction, also breaking momentum conservation. A symmetry known as the KK number, coming from momentum conservation, is therefore also broken by this Z_2 symmetry. But a residual conservation is seen; the KK-parity is given by $(-1)^m$. All modes with odd m will be charged under this parity. It is also clear there will be mixing between KK modes due to this broken momentum conservation. The DM candidate emerging from these modes is

known as the lightest Kaluza-Klein particle (LKP), where $m = 1$ [28]. It was first discussed by Kolb and Slansky, who coined it the pyrgons [29]. The LKP is stable as it is protected by KK-parity, at tree-level. As stated, a DM candidate must be stable, electrically neutral and non-baryonic. The best candidates from this theory then become the first level KK modes of the neutral gauge bosons (the photon and Z boson) and the neutrino. Following the notation of [28], we will refer to the first photon mode as $B^{(1)}$.

Returning to the KK modes, first consider imposing periodic boundary conditions on our orbifold (we consider fields even under Z_2), expanding in Fourier modes gives us particles in the form (suppressing spacetime indices),

$$\psi(x^\mu, x^4) = \sum_{n \in \mathbf{Z}} e^{(inx^4/R)} \phi_n(x^\mu) \tag{11}$$

where the quantisation of the momentum in the extra dimension, x^4, keeps the wavefunction single-valued [30]. Here R is the radius of the orbifold. For completeness, $\phi_n^* = \phi_{-n}$. Using the equation of motion, it can be seen that there are mass modes of $M_n^2 \sim n^2/R^2$, and we have found the tower of KK modes. The other quantum numbers of the particle will remain unchanged. The zero modes here correspond to Standard Model states [27]. A detection of the higher modes, as seen by CERN, would appear as periodic spikes in the number of events as a function of centre of mass energy. So far no such signal has been found.

The relic density of $B^{(1)}$ has been computed in [28], where they considered coannihilations with the next lightest KK particle, $e_R^{(1)}$, the right handed first KK mode of the electron. It can been seen in Figure 4. It was assumed all other modes are too heavy to contribute. The relative mass difference between the LKP and the NLKP was inputted as

$$\Delta = \frac{m_{NLKP} - m_{LKP}}{m_{LKP}} \tag{12}$$

It is important to note that the density of the $B^{(1)}$ is increased when considering $e_R^{(1)}$ than without. This is because the cross section for self-annihilation is larger than the cross-section for coannihilation; the particles will decouple at a similar time with coannihilation as without, and the remaining $e_R^{(1)}$ will decay into $B^{(1)}$. The green region is the required relic density, which corresponds to masses between $0.6 - 1.2$ TeV depending on the model considered.

The first mode of the neutrino, $\nu^{(1)}$ has also been considered as a possible candidate. It satisfies stable, electrically neutral and non-baryonic conditions required from WIMPs. Its relic density has been discussed in further detail in [28].

There are other nuances to consider with these particles, these have been discussed in other papers at length. We have used mostly tree-level consideration, but for a paper on the radiative correction to the mass of the KK particles, see [31]. They consider the fact that the extra dimensions in our theory will violate Lorentz symmetry, giving corrections to the mass beyond tree-level. We would also stumble upon log divergences and interactions between only even or odd KK modes. Further discussion on direct detection can be found in [32]. Recent experimental bounds on R are given by $R \lesssim 40 \ \mu$m [33].
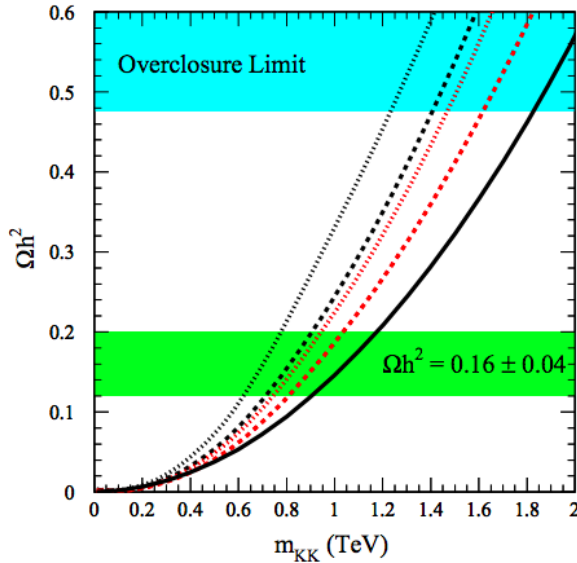
Figure 4: The relic density of $B^{(1)}$ against its mass. The solid line considers $B^{(1)}$ alone, and the dashed and dotted lines correspond to the case in which there are one or three flavors of nearly degenerate $e^{(1)}$ respectively. For each case, the black curves denote the case $\Delta = 0.01$ and the red curves $\Delta = 0.05$. Figure taken from [28].

2.5   Constraints from collider experiments (Davey)

As WIMPs interact very weakly with normal matter, one would assume that trying to find them using high energy particle colliders is unfeasible. However, finding indications dark matter is one of the big aims of the LHC. Although dark matter most likely can not be directly detected in a collision experiment, it is possible to see the effects of dark matter. As the direct WIMP searches depend on a strong coupling of WIMPs to nucleons, it is expected for these WIMP models that they will also be produced in great numbers in high energy hadron-hadron collisions. In proton-proton collisions transverse momentum p_T and transverse energy E_T, transverse meaning perpendicular to the beam line, need to be conserved. As nowadays the standard model and experimental background are well understood, it is possible to reconstruct the collision from the data, and thus to find indications of dark matter in the form of missing transverse energy and momentum. Applying a multitude of dark matter models to these possible signatures then in turn constrains the parameter space of these models, which can narrow the search range for direct and indirect detection experiments and also rule out possible signals from these experiments.[34] An example of this can be found in [35], where the model of constrained Minimal Supersymmetric Standard Model(cMSSM) is ruled out using observational data and experimental data from the LHC.

In the case of SUSY, which is thought to be the most natural extension to the Standard Model, 105 new parameters are added to the SM, which are far too many to be able to make any significant constraints. For this reason the models are simplified greatly until only a few parameters remain. Creating random values for these parameters and then fitting them to ATLAS data rules out a lot of models already,

an example of which is shown in 5, where the results of 22 separate ATLAS searches are applied to constrain the parameter space of the phenomenological MSSM model.

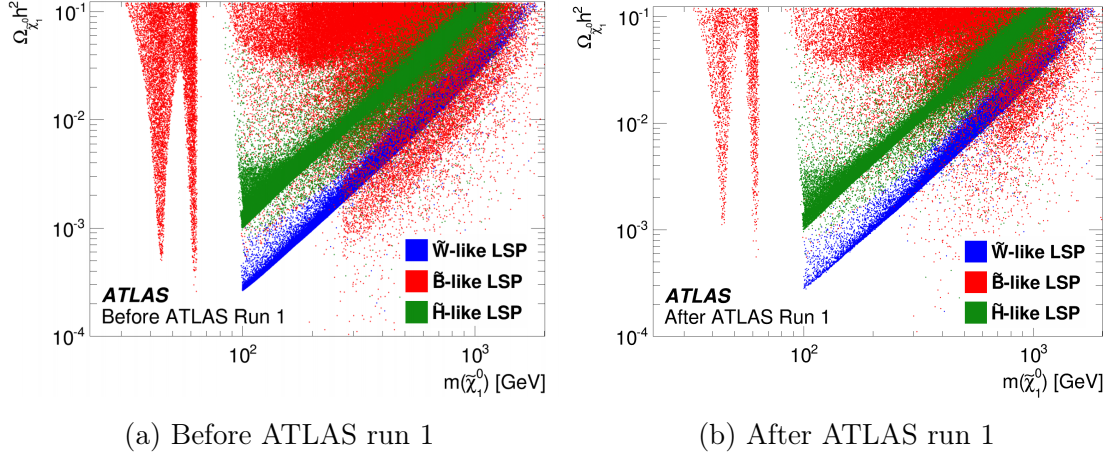(a) Before ATLAS run 1   (b) After ATLAS run 1

Figure 5: The density of pMSSM models for dark matter relic density versus LSP mass, before and after constraints from ATLAS results. Taken from [36].

3 Non-WIMPs

3.1 Sterile neutrinos (Gabriël)

3.1.1 Motivation for sterile neutrinos

Neutrinos are the only electrically neutral, long-lived particles in the Standard Model. The discovery of neutrino oscillations [37, 38] proved that neutrinos have mass. It was therefore widely thought that neutrinos would make up DM. A background of DM neutrinos would be created by means of a freeze out, exactly as discussed in section 2.2. In order for neutrinos to play the role of DM, the sum of the masses of all neutrino flavours should be about 11.5 eV [39]. This is clearly not the case, as it is in conflict with experimental results. The sum of neutrino masses has been determined to be below 2 eV in β-decay experiments [40] while cosmological data provides an upper bound of 1.3 eV at 95% CL [41]. Another constraint comes from the fact that neutrinos are fermions. Due to the Pauli exclusion principle, the phase space density of neutrinos cannot exceed the density of a degenerate Fermi gas. This puts an lower bound on the mass called the *Tremaine-Gunn* bound [42] which is a few hundreds of eV for dwarf galaxies and a few tens eV for galaxies [39]. Following these arguments, the SM neutrino cannot be a viable DM candidate.

A straightforward extension of the electroweak part of the Standard Model (SM) is the addition of right-handed neutrons, or sterile neutrinos [43]. They are the hypothetical RH chiral counterparts of the LH neutrinos of the SM. Adding sterile neutrinos to the SM results in massive neutrinos therefore sterile neutrinos naturally explain neutrino flavour oscillations [39]. Since they are electrically neutral and right-handed, they are singlets under $SU(2) \otimes U(1)$: they do not take part in weak or electromagnetic interactions. They only interact with matter through mixing with active neutrinos. Sterile neutrinos not only naturally explain neutrino oscillations,

they could also provide an explanation for the observed baryon asymmetry in the Universe [44]. They are therefore a very popular extension of the SM. To explain the two observed mass splittings ($\Delta m_{\mathrm{sol}}^2$, $\Delta m_{\mathrm{atm}}^2$) in neutrinos in the SM, at least two additional sterile neutrinos are needed. But to also account for the observed DM today, it was shown that the minimal number of sterile neutrinos is 3 [44]. This model is called the *Neutrino Minimal Standard Model* (νMSM) model. νMSM solves three major problems for beyond the SM models [39]:

- Neutrino flavour oscillations

- The absence of primordial antimatter

- Dark matter

3.1.2 Production in the early Universe

Sterile neutrinos are neutral, long-lived and potentially massive particles and would therefore make an excellent DM candidate. But to be a viable DM candidate, sterile neutrinos also need to be produced efficiently in the early Universe.

A logical thought would be that a relic sterile neutrino denisty would also be produced in freeze out in the early Universe. Since sterile neutrinos are fermions as well, the Tremaine-Gunn bound on the mass of the sterile neutrino is the same as for ordinary neutrinos: 0.4 keV [45]. Sterile neutrinos also have the same number density in equilibrium as ordinary neutrinos (112 cm^{-3}). Using these numbers the energy density today would be $\rho_{\mathrm{sterile,eq}} \simeq 45$ keV/cm^3 [45]. This is considerably larger than the critical energy density of the Universe. Sterile neutrino DM can therefore not be produced in a thermal freeze out.

Sterile neutrinos only interact with SM neutrinos via mixing, but this mixing is strongly suppressed at temperatures above a few hundred MeV [43]. Therefore DM sterile neutrinos are never in thermal equilibrium with the cosmological plasma and their number density is significantly smaller than that of active neutrinos. This is also the reason that they can account for DM without violating the Tremaine-Gunn bound. Sterile neutrinos are an example of decaying DM. Through its mixing with the ordinary neutrinos, a sterile neutrino can decay via Z boson exchange into three (anti)neutrinos [46], as shown if figure 6a.

The total decay width for $N \rightarrow 3\nu$ is given by [45]:

$$\Gamma_{N\rightarrow 3\nu} = \frac{G_F^2 m_N^5}{96\pi^3}\sin^2\theta = \frac{1}{4.7\times 10^{10}\ \mathrm{sec}}\left(\frac{m_N}{50\ \mathrm{keV}}\right)^5\sin^2\theta, \tag{13}$$

where G_F is the Fermi constant, m_N is the mass of the sterile neutrino and θ is the mixing angle. To be DM, the lifetime of the sterile neutrino should be larger than the lifetime of the Universe. This puts constraints on the mixing angle θ:

$$\theta^2 \lesssim 1.1\times 10^{-7}\ \left(\frac{50\ \mathrm{keV}}{m_N}\right)^5 \simeq 34.4\ \left(\frac{\mathrm{keV}}{m_N}\right)^5 \tag{14}$$

Besides the decay via a Z boson, sterile neutrinos can also decay into an active neutrino and a photon, see figure 6b.The total decay width for $N \rightarrow \gamma\nu$ is given by [46]:
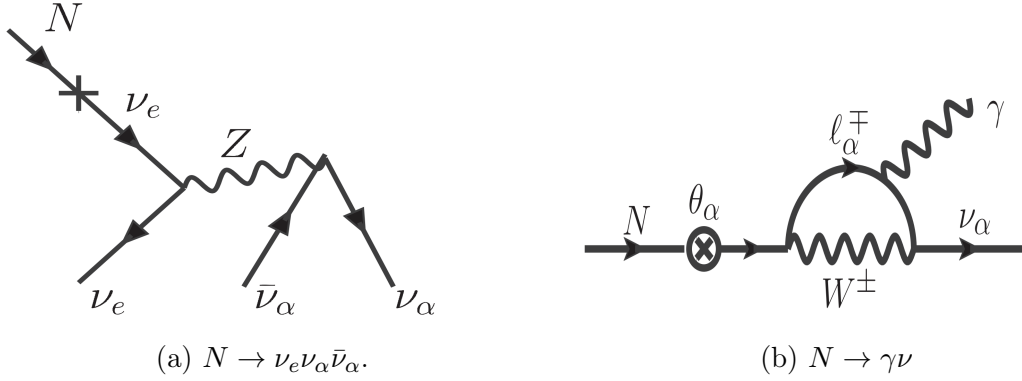
(a) $N \to \nu_e \nu_\alpha \bar{\nu}_\alpha$.

(b) $N \to \gamma \nu$

Figure 6: Left: Decay of sterile neutrino $N \to \nu_e \nu_\alpha \bar{\nu}_\alpha$ through neutral current interactions. A virtual ν_e is created and the quadratic mixing angle (marked by the symbol "×") is proportional to θ^2. Right: Two-body decay of sterile neutrino. The energy of the photon is $E_\gamma = \frac{1}{2} M_N$. Figures taken from [39].

$$\Gamma_{N \to \gamma \nu} = \frac{9 \alpha G_F^2 m_N^5}{1024 \pi^4} \sin^2 2\theta = 5.5 \times 10^{-22} \theta^2 \left(\frac{m_N}{\text{keV}}\right)^5 s^{-1}, \tag{15}$$

where α is the fine-structure constant. This puts a significantly stronger constraint on the mixing angle:

$$\theta^2 \lesssim 1.5 \times 10^{-5} \left(\frac{\text{keV}}{m_N}\right)^5 \tag{16}$$

From equation 14 and 16 follows that if θ is sufficiently small, sterile neutrinos are produced non-thermally. In the νMSM dark matter sterile neutrinos are produced in the early Universe via mixing with active neutrinos. The fraction of energy of the present Universe from the sterile neutrino energy is [44]

$$\Omega_N h^2 \sim 0.1 \sum_i \sum_{\alpha=e,\mu,\tau} \left(\frac{|\theta_{\alpha i}|}{10^{-8}}\right)\left(\frac{m_i}{1 \text{ keV}}\right), \tag{17}$$

where $\sum_i$ is the summation over the sterile neutrino N_i. As the production mechanism of sterile neutrinos is the oscillations between active and sterile neutrinos, there exists a resonance, analogous to the Mikheyev-Smirnov-Wolfenstein resonance for neutrino flavour oscillations [47]. For non-resonant production (NRP), the active-sterile neutrino mixing has a peak at [39]

$$T_{\text{peak}} = 130 \left(\frac{m_i}{1 \text{ keV}}\right)^{1/3} \text{MeV}, \tag{18}$$

resulting in "warm" DM particles. Resonant production (RP) of sterile neutrino DM occurs in the presence of lepton asymmetry and results in much colder DM. To account for the observed DM the lepton asymmetry is about $\eta \sim 10^{-6}(\frac{\text{keV}}{m_N})$, which is much larger than the observed baryon asymmetry ($\sim 10^{-10}$)[39]. RP sterile neutrino DM is fully compatible with astrophysical and cosmological observations, but also "warm" enough to suppress substructures in Milky-Way-size galaxies [45].

3.1.3 Searches for DM sterile neutrinos

Figure 7 shows the constraints on the parameter space for DM sterile neutrinos in the νMSM model from cosmological experiments. The phase-space density constraints are related to the Tremaine-Gunn bound for sterile neutrinos, as discussed above. The X-ray constraints are duo to the fact that sterile neutrinos are an example of decaying DM. Their decays therefore produce a narrow line in spectra of DM-dominated astrophysical objects. Many experiments such as XMM-Newton, Chandra, INTEGRAL and Suzaku aimed to discover these lines. None revealed any candidate lines in the $\sim$ 0.5 keV -10 MeV energy range [46]. The Lyman-α bounds come from power-spectrum constraints from the CMB (for a review on the Lyman-α bounds, see [48]).
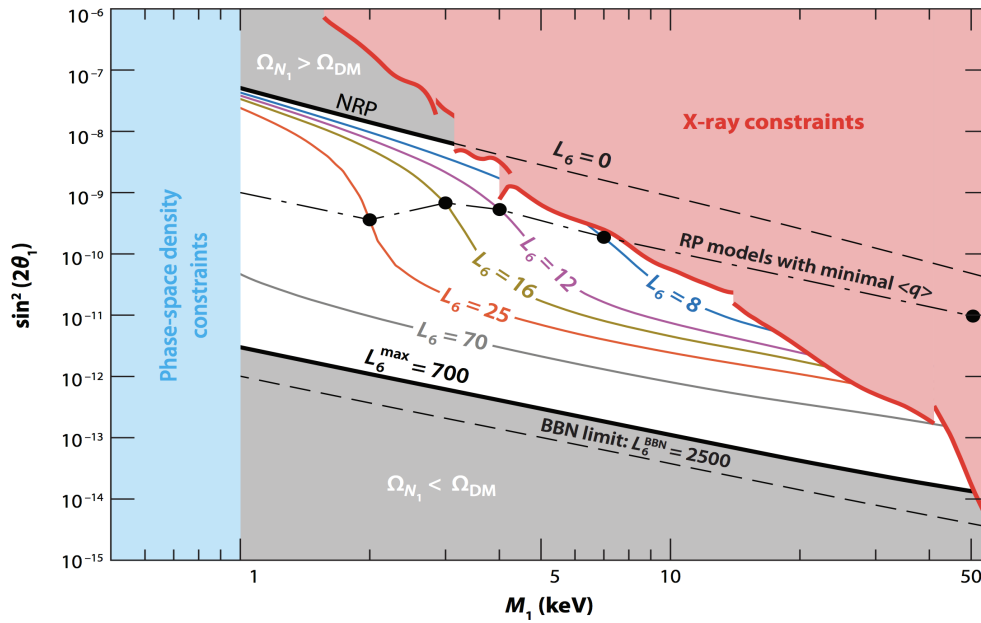

Figure 7: The allowed region of parameters for dark matter sterile neutrinos produced via mixing with active neutrinos (*unshaded region*). The two thick black lines bounding this region represent production curves for non-resonant production (NRP) and resonant production (RP). The red shaded region in the upper right corner represents X-ray constraints. The thin colored curves between thick black lines represent the production curves for different values of lepton asymmetry. The black filled circles are compatible with Lymann-α bounds and the X-ray bounds. The region below 1 keV is ruled out according to phase-space density arguments. Figure taken from [46].

Besides astrophysical and cosmological searches, accelerator experiments also aim to find sterile neutrinos. If the masses of sterile neutrinos responsible for neutrino oscillations are below the electroweak scale, as in the mMSM, they could in principle be found accelerator experiments [39]. These experiments use two strategies. The first is to detect the appearance of the decay products of sterile neutrinos. Properties of such decays can be found in [49]. The second strategy is to investigate the kinematics of rare meson decays [50].

Current data from astrophysical, cosmological and accelerator searches can be described by sterile neutrino DM. Future cosmological research will hopefully detect

the imprints that sterile neutrino DM leaves in power spectra, while accelerator experiments hopefully find hints for sterile neutrino decays.

3.2 Axions (Samuel)

In this section the axion, a hypothetical particle, will be discussed. It was introduced by Roberto Peccei and Helen Quinn in 1977 [51] as a solution to the strong CP problem. Later it was regarded as a possible dark matter candidate, due to its collisionless and non-relativistic behavior [52]. Some axion experiments are currently running, yet the searches have not resulted into finding these almost *invisible* particles.

3.2.1 Strong CP problem

The strong CP problem originates from the QCD gauge symmetry due to its non-Abelian nature [52]. In QCD the gauge invariant vacuum state can be written as

$$|\theta\rangle = \sum_n \mathrm{e}^{in\theta}|n\rangle \tag{19}$$

where θ is a parameter that describes the vacuum state $|\theta\rangle$. This θ can be interpreted as an angle, yet it is not invariant under transformation $\theta \to \theta - \sum_{i=1}^{N} \alpha_i$ and hence not observable [52]. However, $\bar{\theta} \equiv \theta - \arg \det\mathcal{M}$, with $\mathcal{M}$ the quark mass matrix, is invariant and thus an observable.

The discrete symmetries imposed by the charge and parity operations are violated by the vacuum angle θ in QCD. In opposite to the expectation, CP violation is not observed in QCD. If there is CP violation present in QCD, the most simple observed consequence is an electric dipole moment for the neutron. This can be expressed as $|d_n| \approx 10^{-16}\bar{\theta}e$ cm, with e the electric charge. Currently, the limit on the dipole moment is determined experimentally at $|d_n| < 3.0 \times 10^{-26}e$ cm [53], implying $|\bar{\theta}| < 10^{-9}$. It is not expected for θ to be this small. Moreover, CP violation occurs due to complex quark masses and therefore, it is expected to have θ to be of the order 1 [52]. This discrepancy is called the strong CP problem. The question remains why θ is very small, while CP violation is present in the Standard Model.

3.2.2 The Peccei-Quinn solution

In 1977, Peccei and Quinn provided a solution to the strong CP problem. The parameter $\bar{\theta}$ is not interpreted as a parameter, yet plays the role of a dynamical variable [52]. The potential for this variable has a minimum and the variable naturally relaxes to the minimum of this potential. Hence, the value for θ is small. In order to incorporate the PQ solution, a spontaneously breaking global symmetry, $\mathrm{U}(1)_{PQ}$ is necessary [54]. This symmetry replaces the CP violating angle $\bar{\theta}$ by a dynamical charge-parity conserving field. The implementation of this symmetry results in the existence of a Nambu-Goldstone boson, the axion, and $\bar{\theta}$ can be absorbed into its field a [52]. Moreover, non-perturbative effects make QCD depend on $\bar{\theta}$, which provides a potential for the axion, through which the axion obtains mass. The axion slides down to the potential's CP conserving minimum, the solution to the strong CP problem.

3.2.3 Axions as dark matter candidates

Axions are a proper dark matter candidate for the following reasons:

1. Axions are non-relativistic (cold)

2. The population of axions could be present in sufficient quantities to provide the required energy density for dark matter

3. Axions are almost collisionless, only long-range interaction is gravity

The mass of the axion m_a is found to be around $26.2 \pm 3.4 \mu$eV [55]. Nevertheless, the cold axions are produced from equilibrium. There are three different mechanisms through which cold axions are produced:

1. vacuum realignment

2. string decay

3. domain wall decay

The mechanism that contributes the most to the axion population depends on the inflationary reheating temperature T_R. The axion production incorporates some notions of string theory and topology, which are beyond the scope of this review. For details on axion production through the three mechanisms see for example [56]. Here, only a qualitative overview of axion production is given.

Two important scales are present in axion dark matter production [52]. The first is the PQ symmetry breaking temperature T_{PQ}. The second scale is the temperature at which the axion mass, origination from non-perturbative QCD effects, becomes significant. At high temperatures, QCD effects are insignificant and the axion mass can be neglected [57]. The mass becomes important at critical time t_1, when $m_a t_1 \sim 1$ and the temperature $T_1 \approx 1$ GeV.

At early times and high temperatures (above T_{PQ}) the PQ symmetry is conserved. When the temperature equals T_{PQ}, the symmetry breaks and axion strings appear as topological defects. If T_{PQ} is higher than the inflationary reheating temperature T_R, the axion field is homogenized over large distances and the string density is diluted due to inflation. In opposite, if $T_{\mathrm{PQ}} < T_R$, the axion field is not homogenized through the universe and strings radiate cold axions with zero mass. This process continues until T_1 is reached, when non-perturbative QCD effects become important. When T_1 is reached, the axion strings become boundaries of so called N domain walls. A domain wall is a type of topological defect that occurs in case of symmetry breaking. These walls radiate cold axions rapidly and eventually decay in case $N = 1$, implying $T_{\mathrm{PQ}} > T_R$. If $T_{\mathrm{PQ}} < T_R$, string and wall decay contribute to the axion energy density. If $T_R < T_{\mathrm{PQ}}$ and, in addition, the axion string density is diluted due to inflation, only vacuum realignment will contribute significantly to the axion population.

Vacuum realignment produces cold axions, independent of the inflationary reheating temperature. At T_{PQ}, the amplitude of the axion field can have any arbitrary value. If $T_{\mathrm{PQ}} > T_R$, inflation causes homogenization of the axions and the axion field will have a single value for the whole universe. The axion field has a potential due to non-perturbative QCD effects that cause the axions to oscillate. The oscillations

do not decay due to very small couplings of the axion. Therefore the oscillations contribute significantly to the energy density of non-relativistic dark matter. Thus, cold axions originate from vacuum realignment, independent of the reheating temperature.

3.2.4 Experimental searches

Photon-axion mixing Axions are pseudoscalars and therefore can be produced in photon-photon interactions: $\gamma\gamma^* \to a$, the Primakoff effect. [58]. Photons interact electromagnetically, thus this process implies mixing between photons and axions in an electromagnetic field. In 1983, Pierre Sikivie thought of two ways to detect axions based on the Primakoff effect [59, 60]. The first method consists of a microwave cavity in a very strong magnetic field,

3.3 Fuzzy Dark Matter (Rose)

Another theory for the origin of DM is what is known as Fuzzy Dark Matter (FDM). It is constituted of ultralight scalars, and the theory is posed as an alternative to CDM. It has a mass $m \sim 10^{-22}$ eV and a de Broglie wavelength $\lambda \sim 1$ kpc [61]. While CDM is a well accepted theory for DM, there are several problems with it. Although it predicts large scale effects that are consistent with our observations, the theory cannot account for small scale structures. On galactic scales, although it has not been strictly modeled, naïve predictions yield results that are entirely inconsistent with our observations. They predict core densities larger than observed and a cusp with density $\rho \sim r^{-1}$, which are not observed [62]. The density of dwarf galaxies have a density much lower than predicted from CDM. Obviously, the physics on these scales is very complicated, and the referenced paper allows an explanation in the form of 'baryonic physics'. There is a theory in between CDM and HDM, known as Warm Dark Matter (WDM). The thermal velocity distribution has significant, nonlinear, gravitational effects on structure formation [63]. The large de Broglie wavelength allows allows the FDM to suppress small scale structures while still giving same predictions as CDM for large scale structures.

3.3.1 Light Spin Zero Fields

When the mass and the spin of a particle are exactly zero, there is an additional shift symmetry in the action.

$$S = \frac{1}{2} \int d^4x \sqrt{-g} g^{\mu\nu} \partial_\mu \phi \partial_\nu \phi \tag{20}$$

This symmetry is given by $\phi \to \phi + c$, where c is any constant. However, this symmetry is broken by the introduction of many other terms, for example a mass term in the form $m^2\phi^2$, a potential term, $V(\phi)$ or interaction terms with other fields. While the mass of the scalar must be non-zero to account for the gravitational effects seen by DM particles, we can impose the mass to be very light, giving us an approximate shift symmetry, which we expect to be broken on some level.

However, we could also consider an angular field, taking an action in the form,

$$S = \int d^4x \sqrt{-g} \left(\frac{F^2}{2} (g^{\mu\nu} \partial_\mu a \partial_\nu a) - \mu^4 (1 - \cos a) \right) \tag{21}$$

It is clear to see there is a shift symmetry for $c = 2\pi$. As a is dimensionless, the variable F has been introduced via dimensional analysis. The shift symmetry does allow us to add any higher harmonics, but the value of μ that is required to account for DM effects will cause the coefficients of the higher harmonics to be negligible [61]. These particles can arise naturally from other theories, i.e we see them in theories that weren't designed to predict them. All theories of particle physics derived from string theory contain at least a few of these particles ([64], [65], [66]). For this particle, the mass takes the form

$$m = \frac{\mu^2}{F} \tag{22}$$

and it is required to be $\sim 10^{-22}$. There have been bounds placed on F. The lower bound is approximately 10^{16}, the model independent axion of the weakly coupled heterotic string [67]. The upper bound is given by the Planck mass, giving us

$$10^{16}\text{GeV} \lesssim F \lesssim 10^{18}\text{GeV} \tag{23}$$

The expression for μ is generated by nonperturbative effects from the instanton. A good approximation is [61]

$$\mu^4 \sim M_{pl}^2 \Lambda^2 e^{-S} \tag{24}$$

where S is the action for the instanton and Λ is a suppression of instanton effects due to supersymmetry. These range from

$$10^4\text{GeV} \lesssim \Lambda \lesssim 10^{18}\text{GeV} \tag{25}$$

which is a range of maximal to no suppression. This also gives bounds on S [68], although this is model-dependent. S can also vary with the volume of the cycle, leading to exponential changes in the mass [69].

The equation of motion for these particles is

$$D_\mu D^\mu a + m^2 a - \frac{m^2}{6} a^3 + O(a^6) = 0 \tag{26}$$

now we will show if we can really neglect self-interaction compared to its gravitational effects as claimed. Given a body with ϵ, a dimensionless gravitational potential, we would need

$$m^2 a^3 \gtrsim \epsilon m^2 a \tag{27}$$

or, $a^2 \gtrsim \epsilon$. At the temperature where the field begins to oscillate, T_0, we have $a^2 \sim 1$ [61], $\epsilon \sim 10^{-5}$, the primordial cosmic fluctuations [70]. We see that indeed the condition is satisfied. Since $a \sim R^{-3/2}$, where R is the scale factor of the universe, and $R \sim 1/T$, we see we require $T = 10^{-5/3} T_0$ for gravitational effects to dominate. Given a value $T_0 = 500$ eV, we know that the gravitational effects will dominate in time for the radiation-matter equality, $T_{\Omega_m = \Omega_r} \sim 1$ eV.

Looking at today's universe, we roughly have $\epsilon \sim G\rho L^2 \sim G F^2 m^2 a^2 L^2$, with an object of length L and density ρ. This leaves us with the condition

$$L \gtrsim \frac{\sqrt{G}}{Fm} \tag{28}$$

which is equivalent to saying gravitational effects dominate with sizes larger than 1 pc.

3.3.2 Astrophysical Consequences

To see systems where the self-interaction of the FDM dominates, we must look at smaller scales. This means we can look inside the Milky Way or nearby systems to see the effects of FDM. Also considering, in the CDM model, small scale structures form first, we can look at objects with a large redshift. Let us consider Jean's instability. This occurs when the gas pressure is not large enough to prevent gravitational collapse in interstellar gas clouds [71]. FDM is instable for masses greater than the Jean's mass. The Jeans radius is given by [72],

$$R_J = \frac{2\pi}{k_J} = \left(\frac{\pi^3}{G\rho m^2} \right)^{1/4} = 55 \left(\frac{10^{-22}\text{eV}}{m} \right)^{1/2} \left(\frac{2.8 \times 10^{11} M_\odot \text{Mpc}^{-3}}{\rho} \right)^{1/4} \tag{29}$$

below this scale perturbations are stable and above it the system will behave as CDM. To give a feeling for the magnitude of the de Broglie wavelength, consider

$$\frac{\lambda}{2\text{kpc}} = \left(\frac{10^{-22}\text{eV}}{m} \right) \left(\frac{10\text{km/s}}{v} \right) \tag{30}$$

If we consider v as the Virial velocity in the de Broglie wavelength, $\lambda = \hbar/mv$, we would return the Jeans radius. It follows from the uncertainty principle (up to factors of $\hbar$)

$$R_J \lambda^{-1} \sim 1 \tag{31}$$

and we that R_J is a point of stability, increasing the momentum will allow the particles more spatial freedom. From this condition, we have an approximate bound on the maximum value for r for a self-gravitating system in equilibrium,

$$r \gtrsim \frac{\hbar^2}{GMm^2} \tag{32}$$

This is only an approximate statement but in general it holds. It also gives us a bound on the central density

$$\rho_c \lesssim \left(\frac{Gm^2}{\hbar^2} \right)^2 M^4 \tag{33}$$

The upper limit here is comparable to the observed central densities of dwarf galaxies [73]. Looking at the Jeans scale for a FDM halo gives

$$R_{JH} \sim 3.4 \left(\frac{c_{10}}{f_{10}} \right)^{1/3} \left(\frac{10^{-22}\text{eV}}{m} \right)^{2/3} M_{10}^{1/9} (\Omega_m h^2)^{-2/9} \text{kpc} \tag{34}$$

where $f_{10} = f(c)/10$, $f(c) = c^3/\ln(1+c) - \frac{c}{1+c}$, $c = c/10$ and $M_{10} = M/10^{10} M_\odot$. Making some assumptions, we can see for smaller halos there is no region with $\rho \sim r^{-1}$, and for larger halos the length of the cusps with r^{-1} dependence has been reduced from the Virial radius to R_{JH} [72]. As stated, the difference between the CDM model and FDM model arises when the de Broglie wavelength λ is comparable to the radius of our object.

   If dark matter is FDM, the occupation numbers in galactic halos will be so high the dark matter will behave as a classical field obeying

$$\Box \phi = m^2 \phi \tag{35}$$

Using the Schrödinger-Poisson equation we would find

$$\nabla^2 \epsilon = \frac{4\pi G}{a}\rho_0(|\phi|^2 - 1) \qquad (36)$$

where $\rho_0 = \frac{3H_0^2}{8\pi G} = mn_0$, the mass density of the universe. Solving this equation in the region $0 < x < L$, with boundary conditions $\phi(0) = \phi(L) = 0$, along with an initial density variation at $t = 0$, $\delta\rho = \rho_0 \sin\left(\frac{\pi x}{L}\right) \gg \rho_b$, where $\rho_b = 2.8 \times 10^{11}\Omega_m h^2 M_\odot$ Mpc^{-3} is the background density is modeled in Figure 8 [72]. There is also a CDM simulation plotted with the same initial conditions.
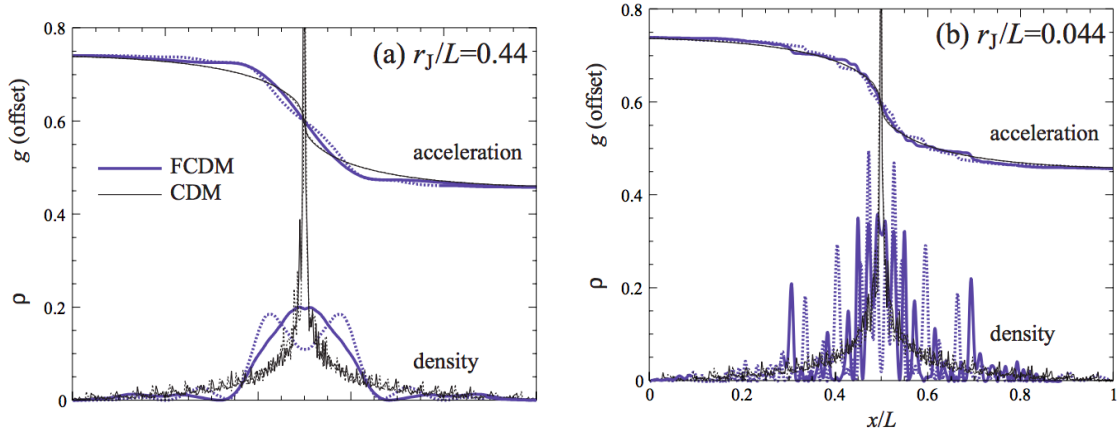

Figure 8: One dimensional simulations (a) large Jeans scale $R_J/L = 0.44$ (b) small Jeans scale $R_J/L = 0.044$. Two snapshots, $t/t_{dyn} = 99$ (solid) and 100 (dotted) are shown for the density profile (units of $15\rho_0$) and gravitational acceleration (units of $3L/2t_{dyn}^2$, offset for clarity). Figure taken from [72].

With the condition $R_J \gg L$, there were no gravitational halos being formed. On the order $R_J \sim L$, we see a gravitational halo but no cusp. We also see a decrease in the core density. For $R_J \ll L$, we see the same effect as the CDM model.

3.3.3 Final remarks

Although one may have concerns about this argument, having bosons with such a light mass may appear unphysical. However, due to the extra symmetry arising from a spinless ultralight scalar coupled to only gravity, it is a very natural argument. This particle would not have been detected from current experiments due to its ultra-light mass. It has been shown that the theory of FDM can suppress the cusps and reduce the core density in cusps. These effects appear to have a cut-off at $r \sim R_J$.

Due to a lack of literature on this topic, this review mostly follows [61] for the physical motivation and [72] for astrophysical consequences. Special thanks to these authors.

3.4 WIMPzillas (Davey)

In most theories of dark matter, dark matter particles are assumed to be thermal relics, particles that were once in local thermal equilibrium in the hot plasma that existed shortly after the Big Bang, until the rate at which they annihilated became

smaller than the rate at which the Universe expanded, leading to the so called dark matter freeze out, after which they were too far apart to annihilate. The reason this theory is so wildly popular is that this puts the expected annihilation cross section of a DM particle nicely on the scale of the weak interaction. However, this puts a limit on the mass of a dark matter candidate, as this annihilation cross section scales inversely with mass, meaning massive particles would need a cross section so low they would be too abundant today. This limit is about $m_{DM} < 34TeV$[74]. So far, no experiments have been able to detect WIMPs or other thermal relics in this expected mass range, opening the door for theories regarding more massive particles. One of these is the so called WIMPzilla, a superheavy particle with a mass above 10^{10} GeV. In this section the general properties, production mechanism as well as one of the major motivations for WIMPzillas will be discussed, starting with the general properties.

3.4.1 WIMPzilla properties

As stated before, the theory of thermal relics puts a limit on the allowed mass of a dark matter candidate. Therefore, if dark matter consisted of WIMPzillas which are far above that limit, they could not have been in thermal equilibrium at the time they decoupled from the hot plasma. Another important criterium for a WIMPzilla is that it needs to be stable or at least have a very long lifetime. As we still observe the effects of dark matter today, the particle that causes these effects needs to be stable enough to have lived to this day. WIMPzillas are also expected to be cold dark matter, as mechanisms to accelerate these superheavy particles to relativistic velocities are unknown as of yet.

3.4.2 WIMPzilla production

While the production mechanism for thermal relics is well understood and dark matter particles arise nicely from it, the production mechanism for nonthermal relics is mostly unknown at the moment. Due to the energy scales needed to produce these superheavy particles, most theories assume the production to happen shortly after the inflationary epoch of the Universe, with the most promising mechanisms being either gravitational production and production during reheating due to inflaton decay. As these theories can be quite complex, only gravitational production will be treated in detail. For production during reheating, see [75][76][77].

Following [78], HERE EXPLAIN GRAVITATIONAL PRODUCTION MODEL(How in depth does this need to be?).

Other exotic production mechanisms like supersymmetry breaking or extra dimensions also exist, for these refer to [79][80][81][82][83].(MORE DETAIL)

Now that one of the production mechanisms for WIMPzillas has been handled, it is time to look at one of the big motivations for WIMPzillas, namely the existence of ultra high energy cosmic rays above the GZK-cutoff.

3.4.3 The GZK-cutoff

In astrophysics, there exists a theoretical limit for the energy of cosmic rays at 5×10^{19}eV, after which these cosmic rays are suppressed. EXPLAIN GENERAL THEORY, MOTIVATION FOR WIMPZILLAS AND CRITICISM.

4 Primordial Black Holes

4.1 Motivation for Primordial Black Holes (Rose)

Due to the extreme conditions of the early universe, they can be considered a breeding ground for Primordial Black Holes (PBHs). PBHs are formed before Big Bang Nucleosynthesis (BBN) and are therefore non-baryonic. Specifically, they are formed when the Schwarzschild radius is comparable to the Hubble radius [84]. Dynamically, they behave as cold objects and are therefore viable candidates for DM. PBHs are also predicted from string theory considering an extra compactified dimension in the braneworld theory [85].

Most candidates for DM require a theory which predicts a new particle, while it is nice to see naturally occuring DM candidates in other theories, each theory often has it's own set of problems and free parameters [22]. A bonus of PBHs are they require no extension to the SM, and they occur naturally in the well-established theory of inflation. They will grow by accreting matter they attract gravitationally.

We can put a number of constraints on the possible masses of these stellar objects. Due to Hawking radiation, they must have a mass which allows the evaporation time to be larger than the Hubble time [86]. The evaporation time is given by $t_{\rm ev} \approx 10^{10}(M_{\rm PBH}/10^{15}{\rm g}){\rm yr}$. Therefore our first constraint takes the form $M_{\rm PBH} > 10^{15}$ g, as any PBH with a lower mass will have evaporated [87].

4.2 Dynamical Constraints (Rose)

Looking at the astrophysical effects of PBHS

References

[1] Leszek Roszkowski, Enrico Maria Sessolo, and Sebastian Trojanowski. WIMP dark matter candidates and searches - current status and future prospects. *Rept. Prog. Phys.*, 81(6):066201, 2018.

[2] Gianfranco Bertone, Nassim Bozorgnia, Jong Soo Kim, Sebastian Liem, Christopher McCabe, Sydney Otten, and Roberto Ruiz de Austri. Identifying WIMP dark matter from particle and astroparticle data. *JCAP*, 1803(03):026, 2018.

[3] Maxim Yu Khlopov. Probes for Dark Matter Physics. *Int. J. Mod. Phys.*, D27(06):1841013, 2018.

[4] David G. Cerdeno. WIMPs: A brief bestiary. In *Proceedings, 4th Patras Workshop on Axions, WIMPs and WISPs (AXION-WIMP 2008): Hamburg, Germany, June 18-21, 2008*, pages 9–12, 2009.

[5] Ken'ichi Saikawa. Axion as a non-WIMP dark matter candidate. *PoS*, EPS-HEP2017:083, 2017.

[6] Yacine Ali-Haïmoud, Ely D. Kovetz, and Marc Kamionkowski. Merger rate of primordial black-hole binaries. *Phys. Rev.*, D96(12):123523, 2017.

[7] Gerard Jungman, Marc Kamionkowski, and Kim Griest. Supersymmetric dark matter. *Phys. Rept.*, 267:195–373, 1996.

[8] George R. Blumenthal, Heinz Pagels, and Joel R. Primack. GALAXY FORMATION BY DISSIPATIONLESS PARTICLES HEAVIER THAN NEUTRINOS. *Nature*, 299:37–38, 1982.

[9] P. Kroupa, B. Famaey, K. S. de Boer, J. Dabringhausen, M. S. Pawlowski, C. M. Boily, H. Jerjen, D. Forbes, G. Hensler, and M. Metz. Local-Group tests of dark-matter Concordance Cosmology: Towards a new paradigm for structure formation? *Astron. Astrophys.*, 523:A32, 2010.

[10] Paolo Gondolo. Non-baryonic dark matter. *NATO Sci. Ser. II*, 187:279–333, 2005. [,279(2003)].

[11] *Supersymmetry, Part I (Theory), Revised by Howard E. Haber* , 2013. http://pdg.lbl.gov/2014/reviews/rpp2014-rev-susy-1-theory.pdf.

[12] N. Arkani-Hamed, A. G. Cohen, E. Katz, and A. E. Nelson. The Littlest Higgs. *JHEP*, 07:034, 2002.

[13] Stefano Profumo. Astrophysical Probes of Dark Matter. In *Proceedings, Theoretical Advanced Study Institute in Elementary Particle Physics: Searching for New Physics at Small and Large Scales (TASI 2012): Boulder, Colorado, June 4-29, 2012*, pages 143–189, 2013.

[14] Scott Dodelson. *Modern Cosmology*. Academic Press, Amsterdam, 2003.

[15] Graciela Gelmini and Paolo Gondolo. DM Production Mechanisms. pages 121–141, 2010.

[16] Gary Steigman, Basudeb Dasgupta, and John F. Beacom. Precise Relic WIMP Abundance and its Impact on Searches for Dark Matter Annihilation. *Phys. Rev.*, D86:023506, 2012.

[17] Nir Polonsky. Supersymmetry: Structure and phenomena. Extensions of the standard model. *Lect. Notes Phys. Monogr.*, 68:1–169, 2001.

[18] H. E. Haber and Gordon L. Kane. The search for supersymmetry: Probing physics beyond the standard model. *Physics Reports*, 117 (2-4):75–263, 1985.

[19] Mohammad Abdullah and Jonathan L. Feng. Reviving bino dark matter with vectorlike fourth generation particles. *Phys. Rev.*, D93(1):015006, 2016.

[20] Kim Griest, Marc Kamionkowski, and Michael S. Turner. Supersymmetric dark matter above the w mass. *Phys. Rev. D*, 41:3565–3582, Jun 1990.

[21] K. Becker, M. Becker, and J. H. Schwarz. *String theory and M-theory: A modern introduction.* Cambridge University Press, 2006.

[22] Gianfranco Bertone, Dan Hooper, and Joseph Silk. Particle dark matter: Evidence, candidates and constraints. *Phys. Rept.*, 405:279–390, 2005.

[23] Thomas Appelquist, Hsin-Chia Cheng, and Bogdan A. Dobrescu. Bounds on universal extra dimensions. *Phys. Rev.*, D64:035002, 2001.

[24] Nima Arkani-Hamed, Savas Dimopoulos, and G. R. Dvali. The Hierarchy problem and new dimensions at a millimeter. *Phys. Lett.*, B429:263–272, 1998.

[25] Bogdan A. Dobrescu and Erich Poppitz. Number of fermion generations derived from anomaly cancellation. *Phys. Rev. Lett.*, 87:031801, 2001.

[26] Lisa Randall and Raman Sundrum. An Alternative to compactification. *Phys. Rev. Lett.*, 83:4690–4693, 1999.

[27] Avirup Shaw. KK-parity non-conservation in UED confronts LHC data. *Eur. Phys. J.*, C75(1):33, 2015.

[28] Geraldine Servant and Timothy M. P. Tait. Is the lightest Kaluza-Klein particle a viable dark matter candidate? *Nucl. Phys.*, B650:391–419, 2003.

[29] Edward W. Kolb and Richard Slansky. Dimensional Reduction in the Early Universe: Where Have the Massive Particles Gone? *Phys. Lett.*, 135B:378, 1984.

[30] David Tong. String Theory. 2009.

[31] Hsin-Chia Cheng, Konstantin T. Matchev, and Martin Schmaltz. Radiative corrections to Kaluza-Klein masses. *Phys. Rev.*, D66:036005, 2002.

[32] Geraldine Servant and Timothy M. P. Tait. Elastic scattering and direct detection of Kaluza-Klein dark matter. *New J. Phys.*, 4:99, 2002.

[33] D. J. Kapner, T. S. Cook, E. G. Adelberger, J. H. Gundlach, Blayne R. Heckel, C. D. Hoyle, and H. E. Swanson. Tests of the gravitational inverse-square law below the dark-energy length scale. *Phys. Rev. Lett.*, 98:021101, 2007.

[34] Felix Kahlhoefer. Review of LHC Dark Matter Searches. *Int. J. Mod. Phys.*, A32(13):1730006, 2017.

[35] Philip Bechtle et al. Killing the cMSSM softly. *Eur. Phys. J.*, C76(2):96, 2016.

[36] Georges Aad et al. Summary of the ATLAS experiment's sensitivity to supersymmetry after LHC Run 1 — interpreted in the phenomenological MSSM. *JHEP*, 10:134, 2015.

[37] Q. R. Ahmad et al. Direct evidence for neutrino flavor transformation from neutral current interactions in the Sudbury Neutrino Observatory. *Phys. Rev. Lett.*, 89:011301, 2002.

[38] Y. Fukuda et al. Evidence for oscillation of atmospheric neutrinos. *Phys. Rev. Lett.*, 81:1562–1567, 1998.

[39] Alexey Boyarsky, Dmytro Iakubovskyi, and Oleg Ruchayskiy. Next decade of sterile neutrino studies. *Phys. Dark Univ.*, 1:136–154, 2012.

[40] C. Patrignani et al. Review of Particle Physics. *Chin. Phys.*, C40(10):100001, 2016.

[41] E. Komatsu et al. Seven-Year Wilkinson Microwave Anisotropy Probe (WMAP) Observations: Cosmological Interpretation. *Astrophys. J. Suppl.*, 192:18, 2011.

[42] S. Tremaine and J. E. Gunn. Dynamical Role of Light Neutral Leptons in Cosmology. *Phys. Rev. Lett.*, 42:407–410, 1979. [,66(1979)].

[43] Scott Dodelson and Lawrence M. Widrow. Sterile-neutrinos as dark matter. *Phys. Rev. Lett.*, 72:17–20, 1994.

[44] Takehiko Asaka and Mikhail Shaposhnikov. The nuMSM, dark matter and baryon asymmetry of the universe. *Phys. Lett.*, B620:17–26, 2005.

[45] M. Drewes et al. A White Paper on keV Sterile Neutrino Dark Matter. *JCAP*, 1701(01):025, 2017.

[46] Alexey Boyarsky, Oleg Ruchayskiy, and Mikhail Shaposhnikov. The Role of sterile neutrinos in cosmology and astrophysics. *Ann. Rev. Nucl. Part. Sci.*, 59:191–214, 2009.

[47] A. Yu. Smirnov. The MSW effect and solar neutrinos. In *Neutrino telescopes. Proceedings, 10th International Workshop, Venice, Italy, March 11-14, 2003. Vol. 1+2*, pages 23–43, 2003.

[48] Alexey Boyarsky, Julien Lesgourgues, Oleg Ruchayskiy, and Matteo Viel. Realistic sterile neutrino dark matter with keV mass does not contradict cosmological bounds. *Phys. Rev. Lett.*, 102:201304, 2009.

[49] Dmitry Gorbunov and Mikhail Shaposhnikov. How to find neutral leptons of the νMSM? *JHEP*, 10:015, 2007. [Erratum: JHEP11,101(2013)].

[50] R. E. Shrock. New Tests For, and Bounds On, Neutrino Masses and Lepton Mixing. *Phys. Lett.*, 96B:159–164, 1980.

[51] Steven Weinberg. A new light boson? *Phys. Rev. Lett.*, 40:223–226, Jan 1978.

[52] Leanne D Duffy and Karl van Bibber. Axions as dark matter particles. *New Journal of Physics*, 11(10):105008, 2009.

[53] P. Schmidt-Wellenburg. The quest to find an electric dipole moment of the neutron. 2016.

[54] R. D. Peccei. The Strong CP problem and axions. *Lect. Notes Phys.*, 741:3–17, 2008. [,3(2006)].

[55] Vincent B.. Klaer and Guy D.. Moore. The dark-matter axion mass. *JCAP*, 1711(11):049, 2017.

[56] Pierre Sikivie. Axion Cosmology. *Lect. Notes Phys.*, 741:19–50, 2008. [,19(2006)].

[57] David J. Gross, Robert D. Pisarski, and Laurence G. Yaffe. Qcd and instantons at finite temperature. *Rev. Mod. Phys.*, 53:43–80, Jan 1981.

[58] H. Primakoff. Photo-production of neutral mesons in nuclear electric fields and the mean life of the neutral meson. *Phys. Rev.*, 81:899–899, Mar 1951.

[59] P. Sikivie. Experimental tests of the "invisible" axion. *Phys. Rev. Lett.*, 51:1415–1417, Oct 1983.

[60] P. Sikivie. Detection rates for "invisible"-axion searches. *Phys. Rev. D*, 32:2988–2991, Dec 1985.

[61] Lam Hui, Jeremiah P. Ostriker, Scott Tremaine, and Edward Witten. Ultralight scalars as cosmological dark matter. *Phys. Rev.*, D95(4):043541, 2017.

[62] David H. Weinberg, James S. Bullock, Fabio Governato, Rachel Kuzio de Naray, and Annika H. G. Peter. Cold dark matter: controversies on small scales. *Proc. Nat. Acad. Sci.*, 112:12249–12255, 2015.

[63] Paul Bode, Jeremiah P. Ostriker, and Neil Turok. Halo formation in warm dark matter models. *Astrophys. J.*, 556:93–107, 2001.

[64] Asimina Arvanitaki, Savas Dimopoulos, Sergei Dubovsky, Nemanja Kaloper, and John March-Russell. String Axiverse. *Phys. Rev.*, D81:123530, 2010.

[65] Shamit Kachru, Renata Kallosh, Andrei D. Linde, Juan Martin Maldacena, Liam P. McAllister, and Sandip P. Trivedi. Towards inflation in string theory. *JCAP*, 0310:013, 2003.

[66] JoAnne L. Hewett and Thomas G. Rizzo. Low-Energy Phenomenology of Superstring Inspired E(6) Models. *Phys. Rept.*, 183:193, 1989.

[67] Kiwoon Choi and Jihn E. Kim. Compactification and Axions in E(8) x E(8)-prime Superstring Models. *Phys. Lett.*, 165B:71–75, 1985.

[68] Peter Svrcek and Edward Witten. Axions In String Theory. *JHEP*, 06:051, 2006.

[69] Renée Hlozek, Daniel Grin, David J. E. Marsh, and Pedro G. Ferreira. A search for ultralight axions using precision cosmological data. *Phys. Rev.*, D91(10):103512, 2015.

[70] D. N. Spergel et al. Wilkinson Microwave Anisotropy Probe (WMAP) three year results: implications for cosmology. *Astrophys. J. Suppl.*, 170:377, 2007.

[71] Volker Bromm, Paolo S. Coppi, and Richard B. Larson. The formation of the first stars. I. The Primordial star forming cloud. *Astrophys. J.*, 564:23–51, 2002.

[72] Wayne Hu, Rennan Barkana, and Andrei Gruzinov. Cold and fuzzy dark matter. *Phys. Rev. Lett.*, 85:1158–1161, 2000.

[73] Shu-Rong Chen, Hsi-Yu Schive, and Tzihong Chiueh. Jeans Analysis for Dwarf Spheroidal Galaxies in Wave Dark Matter. *Mon. Not. Roy. Astron. Soc.*, 468(2):1338–1348, 2017.

[74] Gianfranco Bertone, Dan Hooper, and Joseph Silk. Particle dark matter: Evidence, candidates and constraints. *Phys. Rept.*, 405:279–390, 2005.

[75] Keisuke Harigaya, Tongyan Lin, and Hou Keong Lou. GUTzilla Dark Matter. *JHEP*, 09:014, 2016.

[76] Daniel J. H. Chung, Edward W. Kolb, and Antonio Riotto. Production of massive particles during reheating. *Phys. Rev.*, D60:063504, 1999.

[77] Edward W. Kolb, Daniel J. H. Chung, and Antonio Riotto. WIMPzillas! *AIP Conf. Proc.*, 484(1):91–105, 1999. [,592(1999)].

[78] Daniel J. H. Chung, Patrick Crotty, Edward W. Kolb, and Antonio Riotto. On the gravitational production of superheavy dark matter. *Phys. Rev.*, D64:043503, 2001.

[79] Edward W. Kolb, A. A. Starobinsky, and I. I. Tkachev. Trans-Planckian wimpzillas. *JCAP*, 0707:005, 2007.

[80] Chiaki Hikage, Kazuya Koyama, Takahiko Matsubara, Tomo Takahashi, and Masahide Yamaguchi. Limits on Isocurvature Perturbations from Non-Gaussianity in WMAP Temperature Anisotropy. *Mon. Not. Roy. Astron. Soc.*, 398:2188–2198, 2009.

[81] Daniel J. H. Chung and Hojin Yoo. Isocurvature Perturbations and Non-Gaussianity of Gravitationally Produced Nonthermal Dark Matter. *Phys. Rev.*, D87:023516, 2013.

[82] Sanghyeon Chang, Claudio Coriano, and Alon E. Faraggi. Stable superstring relics. *Nucl. Phys.*, B477:65–104, 1996.

[83] Claudio Coriano, Alon E. Faraggi, and Michael Plumacher. Stable superstring relics and ultrahigh-energy cosmic rays. *Nucl. Phys.*, B614:233–253, 2001.

[84] Bernard J. Carr and S. W. Hawking. Black holes in the early Universe. *Mon. Not. Roy. Astron. Soc.*, 168:399–415, 1974.

[85] Naresh Dadhich, Roy Maartens, Philippos Papadopoulos, and Vahid Rezania. Black holes on the brane. *Phys. Lett.*, B487:1–6, 2000.

[86] S. W. Hawking. Black Holes and Thermodynamics. *Phys. Rev.*, D13:191–197, 1976.

[87] John D. Barrow, Edmund J. Copeland, and Andrew R. Liddle. The Cosmology of black hole relics. *Phys. Rev.*, D46:645–657, 1992.